Coupled Systems Mechanics, *Vol. 15, No. 1 (2026) 17-45*
https://doi.org/10.12989/csm.2026.15.1.017

Techno-Press

Coupled static and dynamic response of functionally graded cracked plates for structural health monitoring

Emad K. Njim*[1], M.R. Al-hadrayi Ziadoon[2], Firas Thair Al-Maliky[3], Adnan A. Alshukri[4], S.M.H. Mohamedhussein[5], Mohsin A. Al-Shammari[6], Royal Madan[7], Kadhim K. Resan[8], Pallavi Khobragade[9]

[1]*Department of Mechanical Power Engineering, College of Technical Engineering, University of Al Maarif, Al Anbar, 31001, Iraq*
[2]*Department of Mechanical Engineering, Faculty of Engineering, University of Kufa, Najaf, Iraq*
[3]*Fuel and Energy Techniques Engineering Department, College of Engineering, AL-Mustaqbal University, 51001, Babylon, Iraq*
[4]*Ministry of Industry and Minerals, State Company for Rubber and Tires Industries, Iraq*
[5]*The General Company for Production of Electrical Power AL-Furat Middle Region Al-Haidarya Power Plant, Najaf, Iraq*
[6]*Department of Mechanical Engineering, College of Engineering, University of Baghdad, Baghdad, Iraq*
[7]*Department of Mechanical Engineering, Graphic Era (Deemed to be University), Dehradun 248002, Uttarakhand, India*
[8]*Materials Engineering Department, College of Engineering, Mustansiriyah University, Iraq*
[9]*Department of civil Engineering, Dev Bhoomi University, Uttarakhand, India*

(Received December 9, 2025, Revised February 17, 2026, Accepted February 20, 2026)

Abstract. This research presents Structural Health Monitoring (SHM) techniques that employ static, modal, harmonic, and transient analyses of functionally graded material (FGM) cracked plates, modeled using First-Order Shear Deformation Theory (FSDT). Crack effects are represented using an equivalent stiffness-reduction method, enabling efficient damage modeling without introducing geometric discontinuities. The study analytically investigates static deflection under concentrated loading, free vibration, harmonic response at resonance, and transient response to impulsive excitation. The primary objective is to predict plate behavior and assess damage history using SHM methodologies, validated by monitoring changes in natural frequencies and dynamic responses of damaged thin plates. Finite element models are developed for cracked steel plates with varying crack lengths and orientations. Results indicate that stress increases with crack length but decreases as the crack orientation aligns more closely with the plate axis (y-axis). Both crack length and orientation significantly influence static compliance, natural frequencies, resonance amplitudes, and transient decay, highlighting the sensitivity of dynamic response parameters to damage severity. The combined use of static and dynamic indicators provides a comprehensive framework for SHM of functionally graded material plates, supporting effective damage detection and integrity assessment. Analytical results exhibit strong agreement with ANSYS simulations, with discrepancies remaining below 1% at a/c=0.01 for all crack angles considered. These findings establish a quantitative relationship between crack parameters and frequency reduction, confirming the model's applicability for vibration-based structural health monitoring of porous FGM plates.

Keywords: finite element method (FEM); functionally graded material (FGM); static analysis; structural health monitoring (SHM); theoretical model; vibration

*Corresponding author, Ph.D., E-mail: emad.kadum@uoa.edu.iq, emad.njim@gmail.com

http://www.techno-press.org/csm/5
ISSN: 2234-2184 (Print), 2234-2192 (Online)

1. Introduction

The interest in the ability to monitor a structure and detect damage at the earliest possible stage is pervasive throughout the civil, mechanical, and aerospace engineering communities. Current damage-detection methods are either visual or localized experimental methods, such as acoustic or ultrasonic methods, magnetic field methods, radiographic methods, eddy-current methods, and thermal field methods [1]. All of these experimental techniques, while effective, are limited by the requirement that the vicinity of the damage is known a priori and that the portion of the structure being inspected is readily accessible. These methods can detect damage on or near the surface of the structure. However, the need for additional global damage-detection methods applicable to complex structures has spurred the development of innovative strategies that examine changes in the structure's vibration characteristics [2]. Structural health monitoring (SHM) is a multidisciplinary scientific field that incorporates computer science, electronics, materials science, and civil engineering [3]. Damage or fault detection, as determined by changes in the dynamic properties or response of mechanical structures, is a subject that has received considerable attention in the literature for its practical applications. The basic idea is that modal parameters (notably fatigue damage) are functions of the structure's physical properties (mass, coupled contact and damage nonlinearities, and stiffness). Therefore, changes in the physical properties will affect the modal properties. While monitoring overall vibrations and dynamic strain measurements for rotating machinery has become a standard practice, attempts to link structural damage to measured modal changes are still in their infancy [4-6]. Several studies have been conducted to address this issue, particularly in the context of buildings and steel structures, using a finite element model (FEM). However, there is a clear need for further development in this area.

Structural Health Monitoring (SHM) technology is a critical technique for ensuring the safe service of composite structures. The major effect limiting the use of composite materials is the lack of understanding of their response and their structural integrity under dynamic loads. Among the prominent damage mechanisms, the debonding under dynamic loading is a well-recognised failure mode for laminated composites [7]. In Zhu et al. [8], a study proposed a data-driven, baseline-free method and experiments to estimate the causes of complex composite structures and detect and characterize structural changes. However, many studies have recently sought to improve damage detection in composite structures [9]. Functionally graded materials (FGMs) are advanced composite materials that have been widely used in recent years due to their attractive mechanical properties, such as strength-to-weight ratios and energy-related applications. As the use of these structures expands into various engineering applications, including aerospace, power plants, aircraft engines, and fusion reactors, the need to understand their behavior becomes increasingly urgent. This understanding is crucial to ensure their regular operation without failure [10-13]. Using a five-unknown high-order shear deformation theory, the bending and free vibration analyses of FG circular plates are explored as a function of various parameters [14].

Bich et al. [15] introduced a practical methodology for detecting and locating damage in a plate structure. This methodology, which utilises damage indices based on changes in the distribution of the plate structure's modal compliance due to damage, has direct and significant applications in structural health monitoring. The changes in the modal compliance distribution are obtained using the mode shapes of the pre-damaged and post-damaged states of the structure, making it a valuable tool for real-world structural assessments. The buckling and free vibration analyses of functionally graded plates are investigated using a trigonometric shear deformation theory [16]. Moreover, the bending and free vibrations of circular plates made of functionally graded material (FGM) are

investigated using a new quadrilateral finite element based on a five-unknown high-order shear deformation theory [17]. Extensive research has addressed the performance and stability of functionally graded material (FGM) structures. For instance, Hemalatha et al. [18] nvestigated transverse wave propagation in functionally graded structures using finite elements with perfectly matched layers and infinite element coupling. Additionally, Alnujaie et al. [19] examined the damped vibration characteristics of functionally graded sandwich beams supported by an advanced viscoelastic foundation model.

The impact of cracks on the dynamic response of bidirectional porous FG beams resting on an elastic foundation is investigated by Dahmane [20]. Also, the fundamental frequencies of cracked FGM beams with the influence of porosity and Winkler/Pasternak/Kerr foundation support are studied using a new quasi-3D HSDT technique [21]. Furthermore, Latroch et al. [22] examined the identification of inclined cracks in bidirectional functionally graded beams supported by an elastic foundation, employing the h-version of the finite element method. In this field, the dynamic characteristics of functionally graded cracked beams resting on a viscoelastic medium are analyzed using a quasi-three-dimensional higher-order shear deformation theory (HSDT). The study is conducted through a series of numerical examples that consider multiple parameters [23].

Based on the principle of stability and performance enhancement, several classical studies on the static and dynamic responses of functionally graded plates have been reviewed to support the current SHM-oriented formulation and demonstrate its application to cracked porous FGM systems [24-26]. Therfore, many studies have investigated the vibration characteristics of cracked functionally graded material plates. The effect of crack location on the vibration analysis of a partially cracked isotropic and FGM microplate with non-uniform thickness is studied using an analytical approach. Green's functions for inhomogeneous fourth-order operators in Rayleigh beams are developed, covering both homogeneous and inhomogeneous cases. It incorporates rotational effects to determine eigenfrequencies, models dynamic vibrations, and computes eigenvalues with first-order corrections for structural analysis [27]. A study compares the roller group and prestress methods for gravity-load simulation in seismic tests using ABAQUS. Results show prestress overestimates restoring force by neglecting P-Delta effects, but the correction significantly reduces errors, improving experimental accuracy [28]. A recent study integrates machine learning with probabilistic learning on manifolds to predict the distributions of seismic responses in reinforced concrete (RC) frame structures. By leveraging key seismic and structural features, this approach achieves high predictive accuracy and enhances both damage assessment and disaster response [29].

Researchers have used analytical, experimental, and numerical (ANSYS) methods to study how fundamental natural frequency affects cracked composite plates under different boundary conditions. Additionally, the impact of a crack in a functionally graded (FG) plate has been analysed analytically under various boundary conditions [30]. Furthermore, the vibration response of sandwich structures under varying boundary conditions, geometrical and material parameters, with and without porosity effects, was performed analytically [31, 32]. According to [33], a closed-form solution is developed for the vibration of a beam with an opening and a closing crack subjected to low-frequency harmonic forcing. The beam was modeled as a bilinear oscillator. Additionally, researchers in [34] performed a numerical investigation of the eigenvalue characteristics and dynamic behavior of damaged porous bidirectional functionally graded (FG) panels.

The intelligent vibration-based structural health monitoring systems, methodological advances and challenges is studied, highlighting recent research advances. A review on vibration analysis of

FGMs' structural components with cracks is conducted by [35]. The effects of cracks and the thermal environment on the free vibration of FGM plates are studied by [36-38]. A hybrid meshless/displacement discontinuity method for a Reissner plate with cracks in FGM is conducted by [39]. Additionally, the radiative energy transfer method is developed to predict vibration energy and stress distribution in functionally graded material (FGM) plates at high frequenciesn [40]. Several recent studies have advanced the understanding of the static and dynamic behavior of FGM structures. Wang et al. [41] studied stiffened FGM plates with cutouts using Nitsche-based isogeometric approach by including FEM. In-plane vibration analysis of elastically restrained FGM skew plates is explored using the variational differential quadrature method [42]. The evaluation of thermal stress intensity factors for an interface crack in FGMs with varying thermal expansion coefficients is analyzed and validated using a multi-region approach [43]. Furthermore, the static deflection behavior of functionally graded beams is examined using multiple beam theories [44]. Finite element analysis of the natural frequencies of a FGM porous cooling plate with cutouts based on a multilayered FGM approach is employed by [45]. Free vibration analysis of multilayer FG plates made of Polyester/Graphene nanocomposites is studied using experimental and Abaqus software tools [46]. Further, the vibration behavior of an imperfect functionally graded material (FGM) cylindrical shell, reinforced with various types of stiffeners and possessing temperature-dependent properties, resting on an elastic foundation, is analyzed [47]. A reduction in porosity weakens the stiffness of structural members; the effect of its distribution on buckling behaviour has been studied [48, 49]. The gradation variation can be unidirectional, bidirectional, or multidirectional, which is imparted to attain directional performance [50, 51].

Numerous studies have shown that vibration-based analysis is a fundamental method in structural health monitoring (SHM) because it is sensitive to damage-induced stiffness degradation. These studies have focused on modeling cracked functionally graded material (FGM) plates using both classical and higher-order theories, emphasizing changes in natural frequencies and mode shapes as indicators of damage. Although crack detection in homogeneous and multilayered plates has been extensively investigated, research on single-phase porous FGMs remains limited, despite their growing application in lightweight, multifunctional structures. The majority of existing work focuses on numerical prediction of dynamic properties, with less emphasis on their relevance for SHM assessment. The present study advances vibration-based modeling by integrating material porosity and crack-induced stiffness reduction within a first-order shear deformation theory (FSDT) framework, providing a physically consistent and computationally efficient method for monitoring the health of FGM plate structures. Nonlinear vibration and dynamic response of functionally graded plates in thermal environments is explored by [52]. Recent studies have examined the impact of longitudinal cracks on the structural lifespan of functionally graded beams with non-linear creep, accounting for various influencing parameters [53].

The studies mentioned above show that considerable research on health monitoring and damage detection has been conducted in recent years. These researchers have developed a wide range of methods to detect structural damage and predict its remaining life. The goal of these methods is to understand the behaviours of the broken plate and determine whether these behaviours can be used for crack detection and health monitoring of structures. The analysis categories include changes in modal frequencies and measured mode shapes (and their derivatives) with the nonlinear method. Finite element models are created and analysed through different analyses. Static, modal, harmonic, and transient analyses are used to analyse the models and extract the responses of cracked plate structures. This study investigates the sensitivity of certain nonlinear vibration

response parameters on geometrically nonlinear vibrations of fully clamped rectangular and square aluminium plates to the presence of damage. The findings, which have significant practical implications, enhance our understanding and prediction of the behavior of structures under harmonic loading with a frequency of excitation close to the first natural frequency, leading to significant amplitude vibrations. Moreover, the study employs an extrapolation method to predict the life and validate the structure through structural health monitoring analysis. The primary objective of this study is to predict the early behaviour of stiffness variation by using structural health monitoring analysis. This aim is achieved by examining cracked and intact plates through static analysis to determine their behaviour under the effect of a concentrated lateral static load. The study also involves exciting the cracked plates using modal analysis to extract natural frequency values for different models and analysing cracked plates with various configurations. Dynamic analyses are employed to estimate responses, offering a comprehensive understanding of model behavior under various loading conditions. Harmonic loads are applied to both cracked and intact plates to evaluate their performance. The research demonstrates practical value, as finite element method (FEM) simulation facilitates crack detection in cantilever plates, thereby enhancing structural safety and efficiency.

Additionally, it uses an impulsive excitation on plate models to extract their time history responses. A crack-sensitive first-order shear deformation theory (FSDT) formulation is presented for functionally graded plates, accounting for crack length and orientation via an equivalent stiffness degradation model. In contrast to conventional FSDT formulations for intact plates, this approach explicitly accounts for crack-induced stiffness loss and its impact on natural frequencies. Analytical predictions are validated against detailed ANSYS simulations, and the results establish quantitative relationships among crack severity, orientation, and frequency reduction. This framework offers computational efficiency for vibration-based structural health monitoring applications.

2. Mathematical formulation of functionally graded cracked plates

2.1 Preliminary concepts and definitions

This study examines functionally graded materials (FGMs), which are composites of metal and ceramic with volume fractions defined by a power-law distribution. The analysis focuses on a plate characterized by length a, width b, and thickness h. A central crack of length 2c is assumed, where c is much smaller than both a and b. The plate is oriented such that it lies in the x-plane, with thickness along the z-direction. The following geometric description is based on these precise crack assumptions:

$$-\frac{a}{2} \leq x \leq \frac{a}{2}, \qquad -\frac{b}{2} \leq y \leq \frac{b}{2}, \qquad -\frac{h}{2} \leq z \leq \frac{h}{2}$$

The material's volume fraction and material properties vary in the thickness direction. According to FGM designs, one of the outer surfaces is metal, and the other is ceramic as shown in Fig. 1. The variations of FGM characterize both plates and beams. According to the following power-law distribution, the FG plate, the ceramic volume fraction (V_c) can be defined as [54].

$$V_c(z) = \left(\frac{z+\frac{h}{2}}{h}\right)^k \tag{1}$$

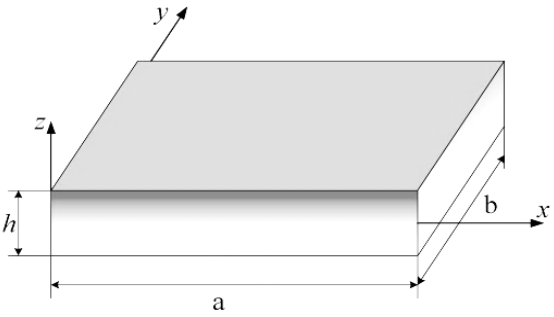

Figure 1. The FG plate model

The volume fraction sum of metal and ceramic is stated as:

$$V_m(z) + V_c(z) = 1 \tag{2}$$

Where (k) represents the volume fraction index. The subscripts (c) and (m) define the composition of metal and ceramic.

The Poisson's ratio ν is assumed to be constant. It is evident from Eq. (2) that the lower surface $\left(z = \frac{h}{2}\right)$ is ceramic-rich, while the top surface $\left(z = -\frac{h}{2}\right)$ is metal-rich, and the rate of the metal constituent in the panel is incremented when (k) rises.

2.2 Theoretical formulation for the free vibration

This section derives the equations of motion based on First-Order Shear Deformation Theory (Mindlin-Reissner plate theory). In this framework, the transverse normal is assumed to deviate from its perpendicular orientation to the mid-surface following deformation. The strain-displacement relationships are expressed by including the von Kármán terms (Pure linear theory) [55, 56].

$$\begin{aligned} u(x,y,z,t) &= u_o(x,y,t) + \mathrm{z}\phi_x(\mathrm{x},\mathrm{y},\mathrm{t}) \\ v(x,y,z,t) &= v_o(x,y,t) + z\phi_y(x,y,t) \\ w(x,y,z,t) &= w_o(x,y,t) \end{aligned} \tag{3}$$

Where u_o, v_o =mid plane displacements, w_o is the transverse displacement, and (ϕ_x, ϕ_y) rotations due to bending about the y- and x axes, while z is the thickness coordinate measured from the mid-surface.

According to FSDT, the linear strain components are given by:

$$\varepsilon_x(x,y,z,t) = \varepsilon_x^\circ(x,y,t) + z\,\kappa_x(x,y,t) \tag{4a}$$

$$\varepsilon_x^\circ = \frac{\partial u_o}{\partial x},\ \kappa_x = \frac{\partial \phi_x}{\partial x} \tag{4b}$$

$$\varepsilon_y^\circ = \frac{\partial v_o}{\partial y},\ \kappa_y = \frac{\partial \phi_y}{\partial y} \tag{4c}$$

And shear strains can be represented by:

$$\gamma_{xy}^\circ = \frac{\partial u_o}{\partial y} + \frac{\partial v_o}{\partial x},\ \kappa_{xy} = \left(\frac{\partial \phi_x}{\partial y} + \frac{\partial \phi_y}{\partial x}\right) \tag{5a}$$

$$\gamma_{xy} = \frac{\partial u_o}{\partial y} + \frac{\partial v_o}{\partial x} + z\left(\frac{\partial \phi_x}{\partial y} + \frac{\partial \phi_y}{\partial x}\right) \tag{5b}$$

Transverse shear strains are given by:

$$\gamma_{xz=}\phi_x + \frac{\partial w_o}{\partial x} \tag{6a}$$

$$\gamma_{yz} = \phi_y + \frac{\partial w_o}{\partial y} \tag{6b}$$

The plate is modeled as a functionally graded material, as shown in Fig. 1, with effective properties varying through the thickness based on a power-law distribution. The material properties are defined as follows:

$$E(z) = E_m + (E_c - E_m)\left(\frac{z}{h} + 0.5\right)^k \tag{7a}$$

$$\rho(z) = \rho_m + (\rho_c - \rho_m)\left(\frac{z}{h} + 0.5\right)^k \tag{7b}$$

Based on Hooke's law, the constitutive relations (plane stress and shear) for a plate may be stated as follow:

$$\{\sigma\} = [\mathrm{Q(z)}]\{\varepsilon\} \tag{8}$$

Where the reduced stiffness matrix is:

$$Q_{11}(\mathrm{z}) = Q_{22}(\mathrm{z}) = \frac{E(z)}{1-\nu^2} \tag{9a}$$

$$Q_{12}(\mathrm{z}) = \frac{\nu\, E(z)}{1-\nu^2} \tag{9b}$$

$$Q_{66}(\mathrm{z}) = \frac{E(z)}{2(1+\nu)} \tag{9c}$$

$$Q_{44}(\mathrm{z}) = Q_{55}(\mathrm{z}) = k_s \frac{E(z)}{2(1+\nu)} \tag{9d}$$

E(z) denotes the effective Young's modulus, and ν is Poisson's ratio. To develop the governing equations, first identify the membrane forces on the FG plates.

By integrating stresses through the thickness yields:

$$N_{ij} = \int_{-\frac{h}{2}}^{\frac{h}{2}} \sigma_{ij}\, dz \tag{10a}$$

And the bending moments:

$$M_{ij} = \int_{-\frac{h}{2}}^{\frac{h}{2}} z\sigma_{ij}\, dz \tag{10b}$$

Furthermore, the transverse shear forces are:

$$Q_x = k_s \int_{-\frac{h}{2}}^{\frac{h}{2}} \tau_{xz}\, dz \tag{11a}$$

$$Q_y = k_s \int_{-\frac{h}{2}}^{\frac{h}{2}} \tau_{yz}\, dz \tag{11b}$$

Where k_s is the factor used to adjust for shear and is given by (k_s =5/6).

The stiffness coefficients include the extensional, coupling, and bending stiffness matrices are:

$$A_{ij} = \int_{-\frac{h}{2}}^{\frac{h}{2}} Q_{ij}(z)\, dz \tag{12a}$$

$$B_{ij} = \int_{-\frac{h}{2}}^{\frac{h}{2}} z\, Q_{ij}(z)\, dz \tag{12b}$$

$$D_{ij} = \int_{-\frac{h}{2}}^{\frac{h}{2}} z^2\, Q_{ij}(z)\, dz \tag{12c}$$

The shear stiffness is:

$$A_{44} = k_s \int_{-\frac{h}{2}}^{\frac{h}{2}} Q_{55}(z)\, dz \tag{13}$$

Hamilton's principle is employed to derive the equations of motion, following the formulation presented by Reddy [57]. The application of this principle is based on the following assumptions:

$$\delta \int_{t1}^{t2} (T - U + W) dt = 0 \tag{14}$$

T represents kinetic energy, U represents strain energy, and W represents external work. The governing equations of motion for the FSDT plate are derived from five coupled in-plane equilibrium equations:

$$\frac{\partial N_x}{\partial x} + \frac{\partial N_{xy}}{\partial y} = I_o \frac{\partial^2 u_o}{\partial t^2} \tag{15a}$$

$$\frac{\partial N_y}{\partial y} + \frac{\partial N_{xy}}{\partial x} = I_o \frac{\partial^2 v_o}{\partial t^2} \tag{15b}$$

The transverse equilibrium can be obtained by:

$$\frac{\partial Q_x}{\partial x} + \frac{\partial Q_y}{\partial y} + p(x, y, t) = I_o \frac{\partial^2 w_o}{\partial t^2} \tag{16}$$

And the rotational equilibrium;

$$\frac{\partial \mathrm{M_x}}{\partial \mathrm{x}} + \frac{\partial \mathrm{M_{xy}}}{\partial \mathrm{y}} - Q_x = I_2 \frac{\partial^2 \phi_\mathrm{x}}{\partial \mathrm{t}^2} \tag{17a}$$

$$\frac{\partial \mathrm{M_y}}{\partial \mathrm{y}} + \frac{\partial \mathrm{M_{xy}}}{\partial \mathrm{x}} - Q_y = I_2 \frac{\partial^2 \phi_\mathrm{y}}{\partial \mathrm{t}^2} \tag{17b}$$

where:

$$I_o = \int_{-\frac{h}{2}}^{\frac{h}{2}} \rho(\mathrm{z})\, dz \tag{18a}$$

$$I_2 = \int_{-\frac{h}{2}}^{\frac{h}{2}} \rho(\mathrm{z})\, z^2\, dz \tag{18b}$$

For the free vibration problem,

$$p(x,y,t) = 0 \tag{19}$$

Assuming harmonic motion

$$\{\Phi\} = \Phi^{\wedge}\,(x,y)\,e^{iwt} \tag{20}$$

The system reduces to the eigenvalue problem:

$$([K] - \omega^2[\mathrm{M}])\{\Phi\} = 0 \tag{21}$$

where: [K] is the global FSDT stiffness matrix, M is the consistent mass matrix, and ω are natural frequencies.

2.3 The static deflection under concentrated load

For a simply supported FGM plate subjected to a concentrated load *P* at the plate center, the governing equation of bending is

$$q(x,y) = P\delta(x - \frac{a}{2}, y - \frac{b}{2}) \tag{22}$$

However, for static loading conditions, the governing equations reduce to the FSDT equilibrium system, which in finite element form is expressed as:

$$[K]\{d\} = \{\mathrm{F}\} \tag{23}$$

where [K] is the FSDT stiffness matrix and {F}represents the equivalent nodal forces due to the concentrated load.

Now, the effective bending rigidity of the cracked FGM plate is

$$D = \frac{1}{(1-v^2)}\int_{-h/2}^{h/2} E(z)z^2.(1-\beta)dz \tag{24}$$

$$E(z) = E_m + (E_c - E_m)\left(\frac{z}{h} + 0.5\right)^k$$

$$\beta = \gamma\,(\frac{a}{c})^2\,\cos\theta_c \tag{25}$$

The maximum static deflection at the plate center is approximated as:

$$w_{max} = \frac{P.a^2}{16\pi^4 D} \tag{26}$$

2.4 Harmonic response analysis (forced vibration)

The harmonic response of the cracked FGM plate under sinusoidal excitation is governed by the reduced dynamic equation

$$M\ddot{q}(t) + C\dot{q}(t) + Kq(t) = F_0 e^{i\omega t} \tag{27}$$

where

$$K \propto D(1-\beta),\ M = \int_{-\frac{h}{2}}^{\frac{h}{2}} \rho(z)\,dz$$

$$\rho(z) = \rho_m + (\rho_c - \rho_m)(\frac{z+h/2}{h})^k \tag{28}$$

The steady-state frequency response function (FRF) is:

$$H(\omega) = \frac{1}{\sqrt{(\omega_n^2 - \omega^2)^2 + (2\zeta\omega_n\omega)^2}} \tag{29}$$

$$\omega_n = \pi^2 \sqrt{\frac{D}{M}} \left(\frac{1}{a^2} + \frac{1}{b^2}\right) \tag{30}$$

2.5 Transient response under impulsive excitation

The transient dynamic response of the cracked FGM plate subjected to an impulsive load is governed by:

$$M\ddot{q}(t) + C\dot{q}(t) + Kq(t) = \delta(t) \tag{31}$$

The analytical solution for an underdamped system is:

$$q(t) = e^{-\zeta\omega_n t} \sin(\omega_d t) \tag{32}$$

With

$$\omega_d = \omega_n \sqrt{1 - \zeta^2} \tag{33}$$

2.6 Crack representation (central crack)

In this approach, the crack is modeled as an equivalent stiffness degradation mechanism instead of a geometric discontinuity, which is especially suitable for vibration-based structural health monitoring. The influence of the crack is incorporated using a dimensionless reduction factor β, defined as a function of the crack length ratio and orientation, and applied directly to the effective bending stiffness terms in the governing equations. This methodology consistently captures the effects of crack severity and orientation on static deflection, natural frequencies, harmonic resonance, and transient responses, while maintaining computational efficiency and numerical stability. Central cracks in plates degrade stiffness locally. For frequency estimation, a practical and widely used approach is equivalent reduced stiffness.

A crack of length a and orientation θ introduces localized compliance, thereby reducing strain energy within the affected region. If the crack affects only a small portion of the plate and does not significantly alter the global deformation mode shapes, the strain energy of the cracked plate can be approximated as follows.

$$U_c(a, \theta_c) \approx U_o \left[1 - \beta(a, \theta_c)\right] \tag{34}$$

Here, β represents the effect of the crack and serves as a dimensionless stiffness-reduction factor that quantifies the relative loss of bending energy due to cracking. This parameter is often calibrated through numerical simulations or experimental procedures.

In vibration-based damage modeling, a crack is typically characterized by a decrease in the structure's capacity to store strain energy, while the mass distribution remains largely unaffected. For thin plates analyzed using First-Order Shear Deformation Theory, the total elastic strain energy associated with bending is given by

$$U_0 = \frac{1}{2} \int_\Omega D\kappa^T \kappa \, d\Omega \tag{35}$$

In this context, Ω denotes the mid-surface domain of the plate, which is the two-dimensional

spatial region occupied by the plate in the x-y plane. D represents the effective bending stiffness of the functionally graded plate, and κ denotes the curvature vector.

Fracture mechanics principles indicate that the reduction in strain energy is proportional to both the crack surface area and its projection along the principal bending direction. Consequently, the parameter β is typically modeled as scaling with the square of the normalized crack length and the directional cosine of the crack orientation. For instance, empirical formulas have been developed to express this relationship.

$$\beta = \gamma \left(\frac{a}{c}\right)^2 \cos^2\theta \tag{36}$$

Here, c denotes the plate characteristic length, and γ represents a calibration constant that accounts for material gradation and porosity effects. In this study, γ is chosen to ensure numerical stability and to align with established trends in the dynamics of cracked functionally graded material (FGM) plates. Additionally, γ is fitted to reference solutions.

The effective bending stiffness is therefore modified as:

$$D_{eff} = (1 - \beta)D \tag{37}$$

which directly influences the governing equations for static deflection, natural frequencies, harmonic response, and transient behavior.

For mode *I* loading in a central crack, The stress Intensity Factor (SIF) is:

$$K_I = \sigma\sqrt{\pi c}.\ f\left(\frac{c}{a}, \frac{c}{b}\right) \tag{38}$$

In numerical analysis (e.g., EEM), model the crack by reducing stiffness in crack zone:

$$E(z) \to \alpha E(z), \text{ with } 0 < \alpha \ll 1 \tag{39}$$

Apply the Alternative Extended Finite Element Method (XFEM) or reduced stiffness modeling to represent enriched functions near crack tips. The parameter α simulates material discontinuity and crack-induced compliance by degrading stiffness. This approach captures local bending rigidity loss without requiring remeshing.

Alternatively, model the crack tip singularity with XFEM, which uses enrichment functions to represent displacement discontinuity and near-tip asymptotic fields. XFEM enables accurate crack modeling without mesh refinement, enhancing computational efficiency and flexibility for crack-propagation studies.

3. Numerical simulation

The finite element model is developed using First-Order Shear Deformation Theory (FSDT), with each node assigned five degrees of freedom: in-plane displacements, transverse displacement, and rotations. The plate domain is discretized using four-node quadrilateral elements to optimize the balance between computational efficiency and accuracy in vibration analysis. Simply supported boundary conditions are imposed along all plate edges to represent a standard structural configuration in vibration-based studies.

The SHELL93 element, an eight-node structural shell, is selected for modeling the material plate. This element effectively represents both curved shells and flat plates, treating flat plates as shells with zero curvature. While supported boundary conditions are implemented in this study, the modeling approach is adaptable to alternative boundary conditions.

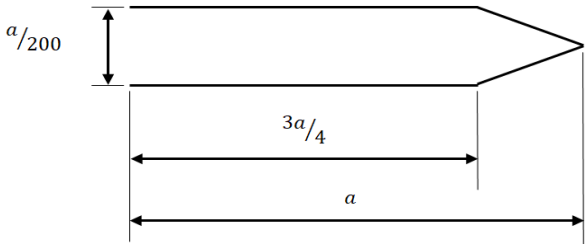

Figure 2. Schematic representation of crack geometry, indicating crack length (a) and orientation (θ)

Each node of the element has six degrees of freedom, comprising translations along the x, y, and z axes and rotations about these axes. The element accommodates quadratic deformation shapes in both in-plane directions and supports analyses involving plasticity, stress stiffening, large deflection, and large strain.

The plate is modeled as a single-phase, functionally graded porous material with mechanical properties varying through the thickness according to a power-law distribution and a defined porosity coefficient. Aluminum is selected as the reference material, and its elastic modulus, density, and Poisson's ratio are specified in the model. Crack effects are simulated by locally reducing the stiffness of elements intersected by the crack region, which captures damage-induced stiffness degradation without introducing geometric discontinuities. This modeling strategy is appropriate for structural health monitoring because variations in global dynamic characteristics can serve as indicators of damage.

Modal analysis is used to determine the vibration characteristics of a structure (natural frequencies and mode shapes). It can also serve as a starting point for harmonic response analysis. The basic equation solved in a typical modal analysis is the classical eigenvalue problem.

The natural frequencies and mode shapes of a structure are important parameters in its design for dynamic loading conditions. The type of crack employed in this study is an open-type crack, with dimensions and form given below, as shown in Fig. 2**.** The figure defines the crack parameters used in the analytical and numerical models. This procedure aims to simulate a cracked plate model. The plate model used includes a central crack with different half- lengths and various crack orientations. The half-lengths of the crack start from (0.015 m) and propagate until (0.12 m) with an increase of (0.015 m). The crack orientations start from (0) and increase by (15) until a vertical position is reached (i.e., 90). Fig. 3 shows the different models where the simulation is made via ANSYS software with the information mentioned above. In the current First-order Shear Deformation Theory (FSDT) formulation, the crack is modeled using an equivalent energy-based stiffness degradation method rather than by introducing an explicit geometric discontinuity.

A reduction parameter, β, is applied to adjust the bending and shear stiffness matrices, such that $D^*=\beta D$ and $A^*=\beta A$. This approach ensures kinematic compatibility and maintains strict compliance with the governing equations derived from Hamilton's principle. However, the analytical model captures global stiffness degradation, whereas the FEM model is used to represent local geometric discontinuities for validation.

4. Results and discussions

A crack-sensitive stiffness-reduction model is integrated into the First-Order Shear

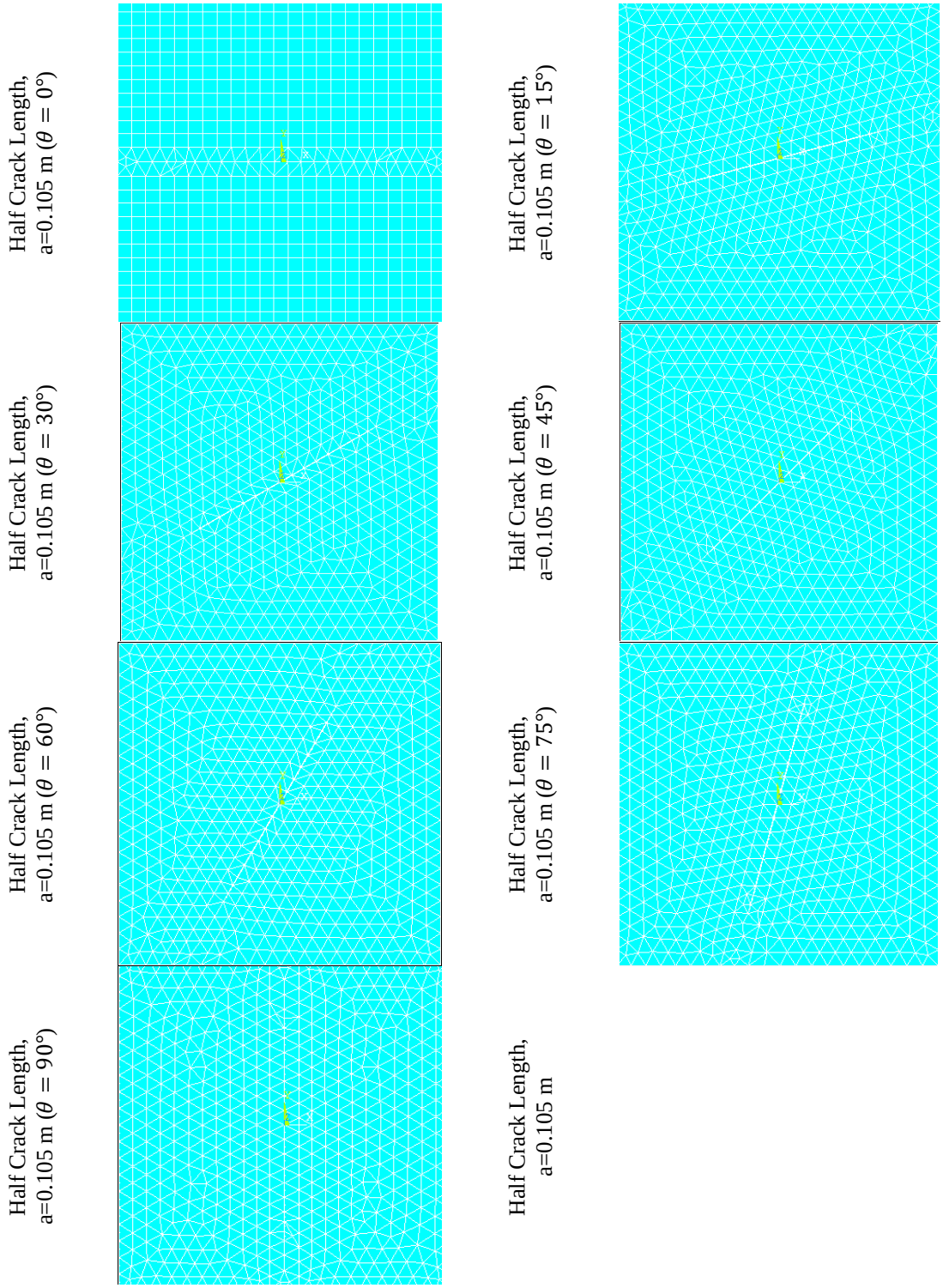

Figure 3. Finite element mesh of the plate with various crack orientations (a=0.105 m), generated using ANSYS. In the numerical model, the crack is modeled as a geometric discontinuity

Deformation Theory (FSDT) framework to quantify the influence of crack length and orientation on modal characteristics.

Analytical solutions (Navier-type) are derived for the free vibration analysis of FGM plates with central crack conditions. The end conditions of the (FGM) thin plate are supported and subjected to the uniform pressure. For the boundary condition considered, it can be written as:

$$w = N_{xy} = \phi_y = 0,\ N_x = N_{x0},\ at\ \ x = 0, a,\ w = N_{xy} = \phi_x = 0, N_y = N_{y0}, at\ y = 0, b \quad (40)$$

4.1 Effect of crack length and orientation

In this study, the free vibration of FG plates with a crack was analyzed using the FSDT plate theory. In addition to free vibration (modal) analysis, the present study incorporates static, harmonic, and transient dynamic analyses to establish a comprehensive framework for structural health monitoring of cracked functionally graded plates. Static analysis quantifies changes in deflection due to damage under concentrated loading. Harmonic response analysis examines resonance behavior and evaluates the sensitivity of frequency response to the presence of cracks. Transient dynamic analysis investigates time-domain displacement responses under impulsive excitation. Collectively, these analyses, together with modal characteristics, offer complementary indicators for damage detection and structural integrity assessment.

To ensure consistency with the study's stated objectives, the numerical investigation is extended beyond free vibration analysis to include static, harmonic, and transient dynamic responses. Modal analysis is used to evaluate crack-induced changes in natural frequencies, while static analysis assesses damage sensitivity by measuring deflection variations under concentrated loading. Harmonic response analysis is used to investigate resonance behavior and frequency response amplitude variations, and transient analysis is conducted to assess time-domain displacement characteristics under impulsive excitation. Together, these analyses provide complementary indicators for vibration- and response-based structural health monitoring of cracked functionally graded plates.

The theoretical results presented in this study are obtained by explicitly incorporating the crack reduction factor β into the effective stiffness matrix, thereby establishing a direct relationship between crack characteristics and measurable changes in the global structural response.

The geometric model is a thin square plate with a central crack of varying length and angle. The dimensions are (30 cm×30 cm) and (1 mm) thickness and the non-dimensional crack length is the ratio between the length of crack and length of plate has the value of 0.1-0.8 increments for each 0.1 (i.e., the smallest crack has the length of 0.015 m and the biggest one has the value of 0.12 m, increased by 0.015 m). Also, it has a different angular orientation of (0° to 90°) with an increase of (15°) as shown in Fig. 4.

The FG plate is taken to be made of aluminum (Al) and alumina (Al_2O_3) with the following material properties:

Ceramic (Alumina, Al_2O_3): E_c=380 GPa, v=0.3, ρ=3800 Kg/m^3.

Metal (Aluminum, Al): E_m=70 GPa, v=0.3, ρ=2702 Kg/m^3.

Numerical results are presented in terms of non-dimensional frequency. The non-dimensional parameter used is:

Fig. 5 illustrates the impact of crack length and orientation on the first-mode natural Frequency of a functionally graded (FG) Al/Al_2O_3 plate. The results reveal that the presence of a crack has a substantial effect on the vibrational response, with this influence being particularly

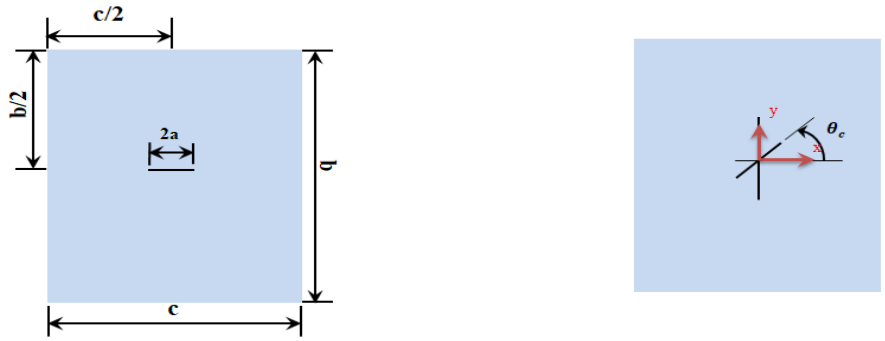

(a) Central crack location (b) Crack orientations

Figure 4. The FG plate geometry (a) Location (b) Orientations of crack

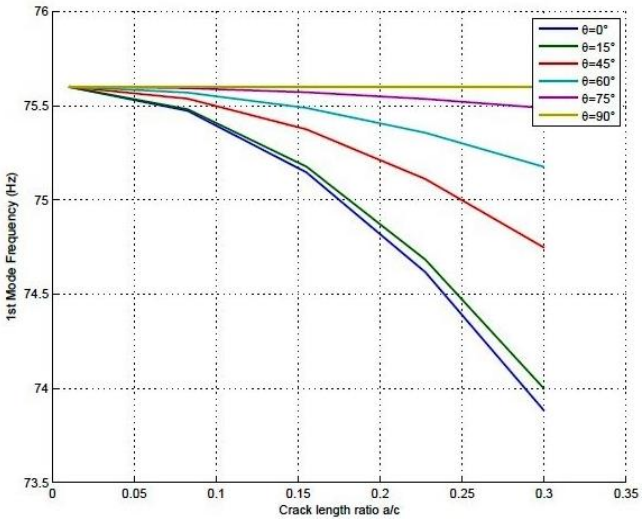

Figure 5. The results of the 1st mode frequency based on various orientations of the a/c ratio

sensitive to both the length and orientation of the crack.

For all orientations except θ=90°, increasing the crack length ratio leads to a noticeable decrease in the first-mode Frequency. This reduction is attributed to the progressive loss of stiffness as the crack length increases, which diminishes the plate's ability to resist deformation during vibration. The Frequency drop exhibits a nonlinear trend, becoming more pronounced for a/c>0.15, indicating accelerated stiffness degradation in this range. However, it's not just the crack length that matters. The orientation of the crack plays a crucial role in the frequency drop. Among the considered orientations, cracks aligned closer to the principal vibration direction (θ=0° and θ=15°) cause the steepest decline in natural Frequency. At these angles, the crack is parallel to the direction of maximum bending strain in the first mode, which maximizes its detrimental effect on load transfer across the plate. The θ=45° orientation results in a moderate reduction, as stiffness loss is distributed in both principal directions, reducing the impact compared to near-parallel cracks.

Cracks at θ=60° exhibit a relatively minor frequency drop, suggesting that oblique orientations

Table 1. The first five natural frequencies [Hz] at each (a (crack length), theta)

a/c	θ_c	1st mode	2nd mode	3rd mode	4th mode	5th mode
0.01	0°	92.7	231.6	231.6	370.6	463.3
0.01	45°	92.7	231.7	231.7	370.6	463.3
0.01	90°	92.7	231.7	231.7	370.6	463.3
0.08	0°	92.5	231.3	231.3	370.0	462.5
0.08	45°	92.6	231.5	231.5	370.3	462.9
0.08	90°	92.7	231.7	231.7	370.6	463.3
0.16	0°	92.1	230.3	230.3	368.4	460.5
0.16	45°	92.4	231.0	231.0	368.5	461.9
0.16	90°	92.7	231.7	231.7	370.6	463.3
0.23	0°	91.5	228.6	228.6	365.8	457.3
0.23	45°	92.1	230.2	230.2	368.2	463.3
0.23	90°	92.7	231.7	231.7	370.6	463.3
0.30	0°	90.6	226.4	226.4	362.2	452.8
0.30	45°	91.6	229.0	229.0	366.5	458.1
0.30	90°	92.7	231.7	231.7	370.6	463.3

Table 2. The first natural frequencies [Hz] according to FSDT and ANYS (percentage difference between FSDT reduced-stiffness model and ANSYS results)

a/c	θ_c	1st mode FSDT	1st mode ANSYS	error
0.01	0°	92.7	92.5	0.22%
0.01	45°	92.7	92.0	0.76%
0.01	90°	92.7	92.8	0.11%
0.08	0°	92.5	90.4	2.27%
0.08	45°	92.6	89.8	3.02%
0.08	90°	92.7	92.5	0.22%
0.16	0°	92.1	87.6	4.88%
0.16	45°	92.4	86.2	6.71%
0.16	90°	92.7	91.3	1.51%
0.23	0°	91.5	85.2	6.89%
0.23	45°	92.1	85.9	6.22%
0.23	90°	92.7	91.1	1.73%
0.30	0°	90.6	85.2	5.96%
0.30	45°	91.6	85.5	6.66%
0.30	90°	92.7	91.4	1.40%

beyond 45° interact less strongly with the dominant bending deformation of the firstmode. The most notable observation is that cracks at θ=75° and θ=90° have minimal influence on the first-mode frequency, even for considerable crack lengths. In these cases, the crack is oriented almost perpendicular to the principal bending axis, and its effect on the load-carrying capability in the first vibration mode is negligible. The material gradation from ceramic-rich to metal-rich regions

in FG (Al/Al_2O_3) plates further modifies the crack's influence, as stiffness asymmetry can alter local deformation fields around the crack tip.

These results underscore the importance of considering crack orientation in damage assessment, particularly in vibration-sensitive applications. While cracks near 90° may be less critical for the first mode, they could still influence higher-order modes or other loading scenarios.

Table 1 presents the first five natural frequencies for *a/c* (0.01-0.3) and θ (0, 45, and 90°). Modal separation remains substantial across all crack ratios. The second and third modes are approximately (150-160%) higher than the first, indicating that higher modes remain dominant despite the presence of cracks. The fourth mode is (60-65%) higher than the second, and the fifth is (24-27%) higher than the fourth, demonstrating consistent modal spacing. While increasing crack length slightly reduces absolute frequencies, it does not significantly affect the percentage gap between modes. This confirms the stability of the modal hierarchy. Overall, cracks mainly influence the magnitude, not the proportional distribution, of modal energy across modes.

The results highlight important considerations for vibration-sensitive applications. FG plates should not be designed with long cracks parallel to the principal vibration direction, as this is critical for nondestructive inspection and damage-tolerance design. Both crack length and orientation must be addressed to maintain structural integrity. These findings align with previous studies on cracked isotropic and FG plates, which show that frequency sensitivity to crack parameters depends on mode shape and crack position.

The comparison between FSDT and ANSYS results presented in Table 2 shows good agreement, with all errors below 7%; indeed, the FSDT model is proven once again. The maximum error of 6.89% appears at a/c=0.23 and θc=0º, which is fairly suitable for engineering purposes. Larger errors are generally observed for longer cracks and 45° orientations, where the structural response is more sensitive. The smallest errors (<1%) are found at low crack ratios, in particular for θc=0º and 90º. In general, the FSDT predictions are in good agreement with ANSYS results, thereby justifying its application for effective vibration analysis of cracked FG plates. These results establish a quantitative relationship between crack parameters and frequency reduction, thereby confirming the model's applicability for vibration-based structural health monitoring of functionally graded material (FGM) plates.

4.2 Effect of power law index k

Fig. 6 illustrates the variation in natural frequencies as a function of the power-law index *k*. As *k* increases, natural frequencies decrease due to a higher metallic volume fraction and reduced bending stiffness. In the context of structural health monitoring, the sensitivity of crack detection with respect to *k* is significant. For a constant crack length ratio (a/c=0.10, θ_c=0°), the relative reduction in frequency increases slightly as *k* increases. These results suggest that plates with higher metal content are more sensitive to crack-induced stiffness degradation. Consequently, material gradation influences both the absolute dynamic response and the detectability of cracks through modal parameters. These findings highlight a crucial design region for customizing vibration performance in FGM structures, offering valuable insights for engineers and researchers in the field.

4.3 Effect of geometrical properties

Fig. 7 shows a 3D surface mode plot for (FG) Al/Al_2O_3 plate at *b*=1.0; theta=45; *a*=0.1 length,

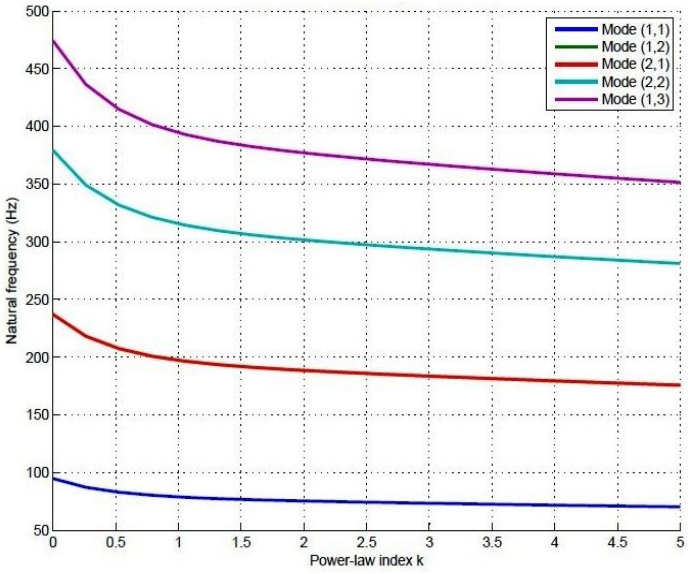

Figure 6. Effect of power-law index on natural frequencies (a/c=0.10, θ_c=0°)

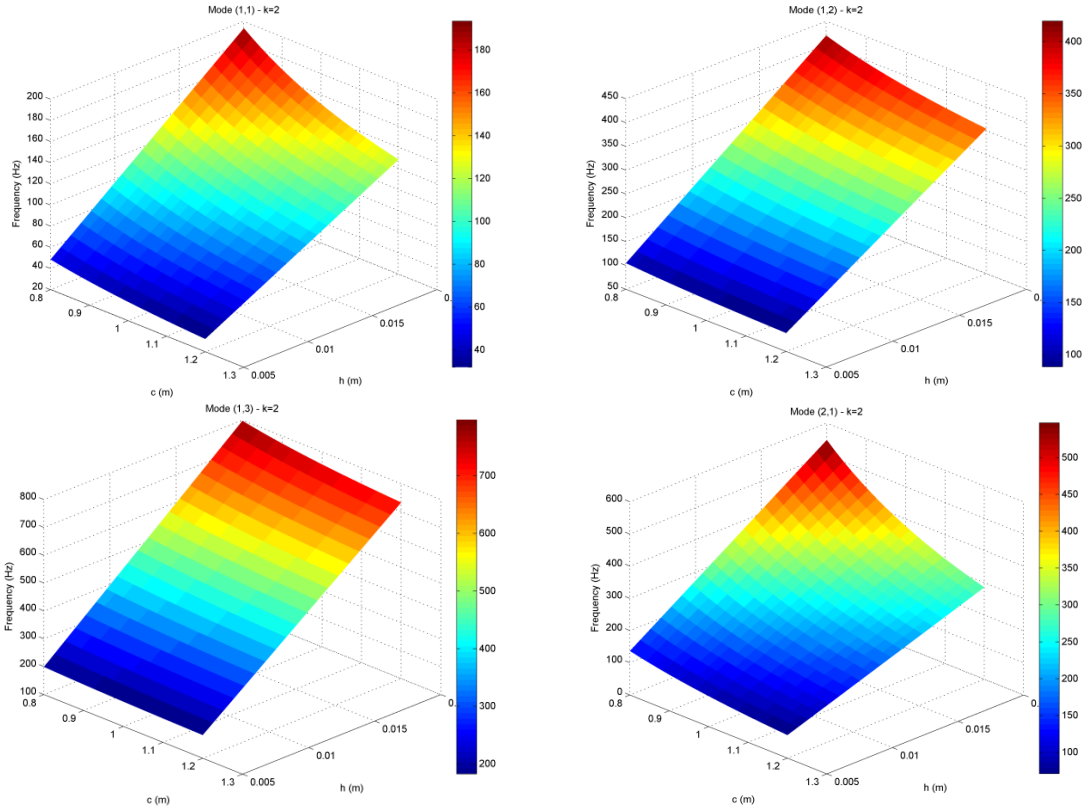

Figure 7. A 3 D surface mode plot for (FG) Al/Al_2O_3 plate at *b*=1.0; theta=45º; a (crack)=0.1 length, and *k*=2 power-law index

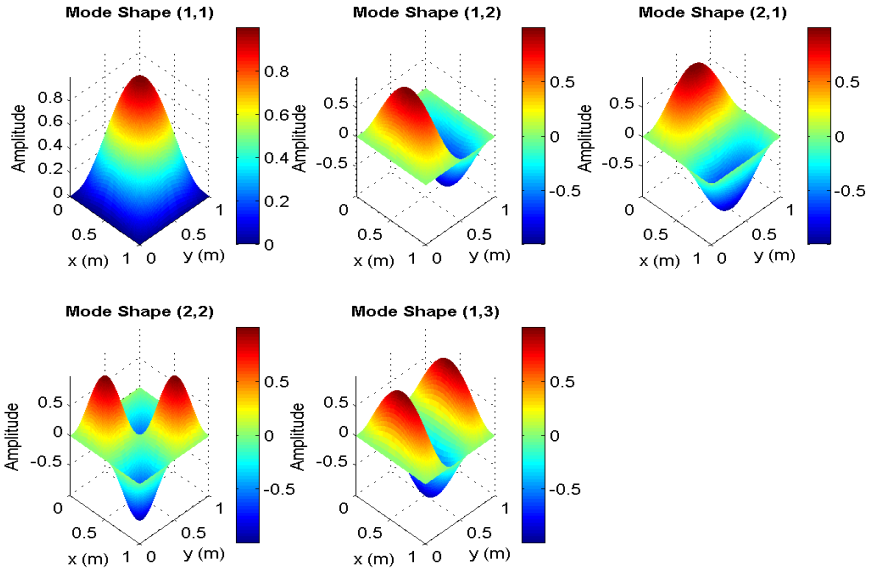

Figure 8. Mode shape plot for CCCC (FG) Al/Al_2O_3 plate at *b*=1.0; theta=45º; a(crack)=0.1 length, and *k*=2 power-law index

and *k*=2 power-law index. It is observed that, with *k*=2 and a fixed crack length a=0.10, increasing the plate width *c* from 0.8 to 1.2 reduces the relative crack ratio a/c, weakening the crack's influence and increasing the natural frequencies. This practical insight can guide engineering researchers in their structural analysis. Furthermore, the study shows that increasing thickness *h* (0.005 to 0.02 m) significantly increases bending stiffness, leading to a pronounced upward shift in all natural frequencies. This finding underscores the practical relevance of thickness as a dominant geometric control. The inclined crack (θ=45º) introduces mixed-mode local flexibility, causing a modest additional Frequency reduction for modes sensitive to shear/torsion compared with θ=0º. However, for *k*=2, the material gradation results in moderate softening, but practical tuning of c and, especially, *h* is more effective at mitigating crack effects and restoring higher vibrational response, providing actionable guidance for structural analysts and materials scientists.

Fig. 8 shows the mode shapes of a cracked FGM plate for five vibration modes. According to the findings, the mode shapes for an FG-cracked plate (modes (1,1) to (2,2) and (1,3)) are obtained, including the deformation shapes and normalized amplitude values. In Mode (1,1), the plate symmetrically oscillates with a single peak amplitude of ~0.88 at mid-span. Mode (1,2) exhibits a single nodal line along the y direction with an oscillating sign of lobes; the maximum amplitude is about ±0.55. The same goes for Mode (2,1); it has a nodal line along the x-axis with a similar amplitude range. In the Mode (2,2), two lines of symmetry nodes divide the plate into four vibrating areas, resulting in a symmetric saddle coordinate shape with amplitudes near ±0.56. Mode (1,3) exhibits three bands along the y-direction, corresponding to higher frequency and complicated vibrations, and its amplitude varies with a maximum of the maximum amplitude ≈ ±0.55. The color maps (blue to red) clearly demonstrate the spatial variation in amplitude across the plate. The mode shapes become more complex, with a greater number of nodal lines as the mode number increases, and exhibit higher sensitivity to crack and geometric effects.

Fig. 9 shows the variation of natural frequencies for a cracked functionally graded (FG) plate

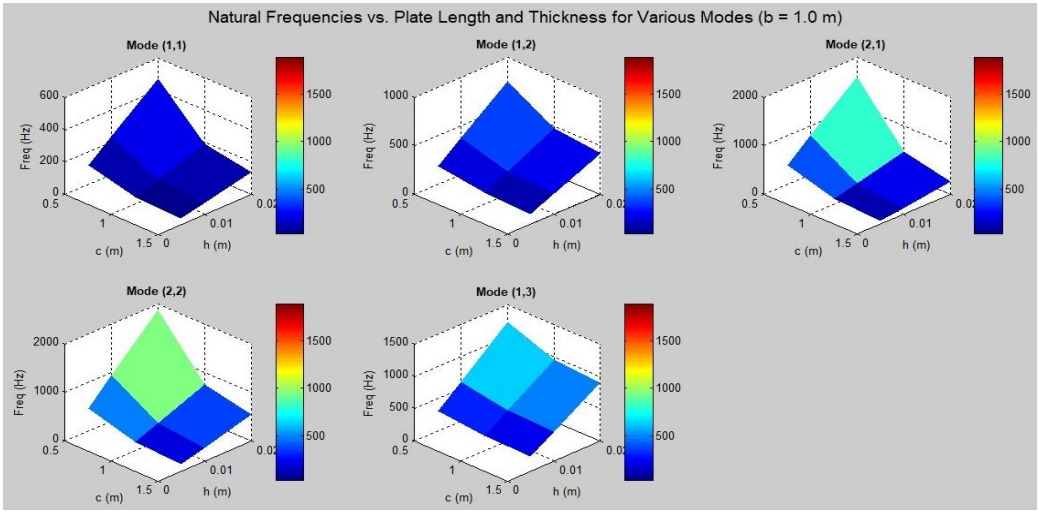

Figure 9. The natural frequencies results vs. FG plate thickness for various modes at b=1.0 m; theta=45º; and k=2 power-law index

with plate thickness (h) and length of the plate (c) for several modes of vibration. The calculations are made considering the fixed values of the plate width (b=1.0 m), the angle of orientation of the crack (θ=45º), and the power-law index (k=2), which represents the material gradient from ceramic to metal. In all cases, the same trend is observed: the resonant frequency increases with increasing plate thickness and decreases with increasing plate length. This is similar to the classical vibration theory, which states that a thicker plate will have a higher flexural stiffness, leading to a higher natural frequency. On the other hand, if the plate length is further increased, the stiffness of the plate is decreased, and therefore, vibration frequencies are decreased. For the fundamental mode (1,1), the modes have the smallest frequencies among the considered modes, up to about 600 Hz. This mode shows a comparably even and slow evolution in the geometry, which indicates low sensitivity to geometrical changes. The natural frequencies become much larger than these, reaching over 2000 Hz in the (2,1) and (2,2) modes as the mode number increases. This increased sensitivity to the geometric parameters and the crack-induced stiffness reduction is revealed by the fact that these higher-order modes exhibit steeper slopes in the frequency response surfaces. The crack influence, modeled under a 45º angle in the model, represents localized stiffness reduction and "anisotropic stress fields", or stress fields where the magnitude and direction depend on the direction of the material. This leads to a general reduction in frequencies compared to their uncracked counterparts.

It is more significant in higher modes due to more complicated mode shapes and relatively higher strain energy concentrated around the crack. The material properties used for the FG materials with k=2 result in a non-homogeneous distribution of the material in the plate thickness direction, with the material transitioning from ceramic at the top to metal at the bottom. Stiffness distribution and mass density, which affect the dynamic response, are influenced by gradual changes in these constituents. At k=2, the plate has greater metal content (relative to ceramic), leading to an overall decline in stiffness compared to lower k values (such as near-ceramic geometries). Consequently, the natural frequencies derived are smaller than those of fully ceramic plates and larger than those of metal plates, which are the intermediate characteristic of FGMs.

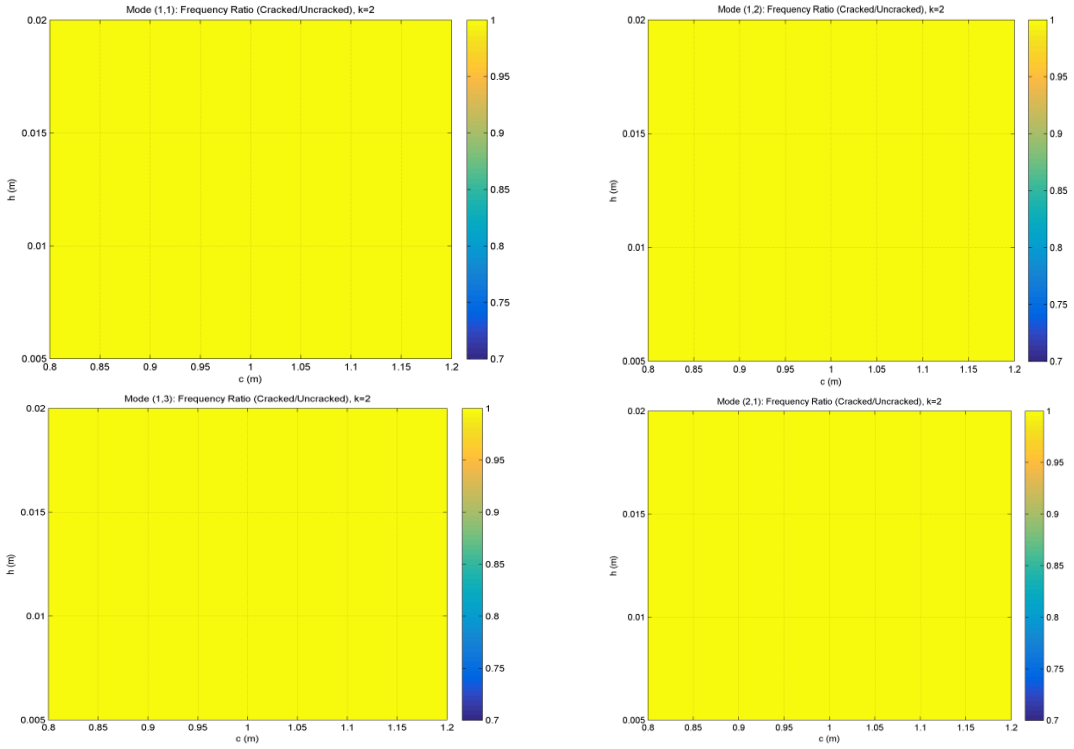

Figure 10. The frequency ratio (cracked/uncracked) results for the FG plate at a (crack)=0.1 crack length b=1.0 m; theta=45º, and k=2 power-law index

Incompletely, the findings directly reveal the synergistic influences of geometry, crack direction, and material property configuration on the dynamic behaviour of FG plates. This work offers useful information for the design and vibration suppression of cracked FG structures, particularly when stiffness and frequency tuning are required, as in aerospace, mechanical, and civil engineering systems, thereby highlighting the significance of the present work in these fields.

Fig. 10 illustrates the frequency ratio ($f_{cracked}/f_{uncracked}$) as a function of crack length ratio and orientation. For minimal crack lengths (a/c≈0.01), the ratio remains near unity, which suggests negligible stiffness degradation. As crack length increases, the frequency ratio decreases monotonically, thereby confirming progressive loss of bending stiffness. The deviation from unity is more significant for certain crack orientations. These results demonstrate that modal parameters are highly sensitive to both crack severity and orientation, which supports their application in structural health monitoring.

The response is the same for modes (1,1), (1,2), (1,3), (2,1), and (2,2), indicative of robust vibrational stability. Negligible sensitivity to crack presence is verified by the uniform yellow color around the contour. These results demonstrate the remarkably high damage resistance during dynamic loading in FG plates and support the potential of FG as a reinforcement material in structural applications.

Mode I SIF estimation from the displacement field is shown in Fig. 11. The true (simulated) KI is 1.000e+06 Pa√m, and the estimated is 1.000e+06 Pa√m (CR=1.000). The estimated mode I SIF (KI) and the true (simulated) KI have been plotted based on the displacement field near the crack

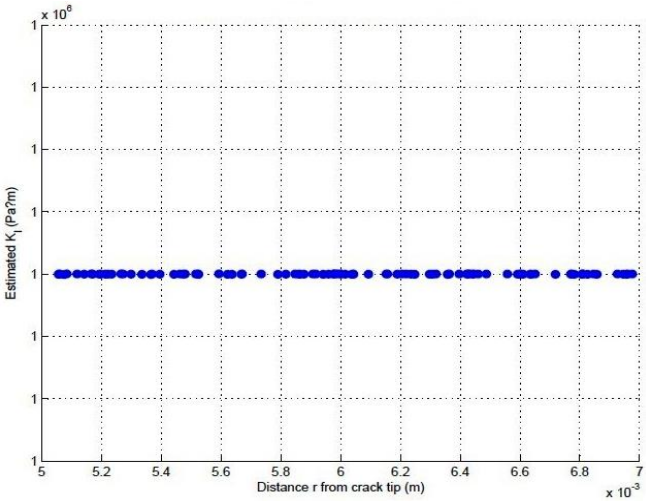

Figure 11. The mode I (SIF) estimation from the displacement field

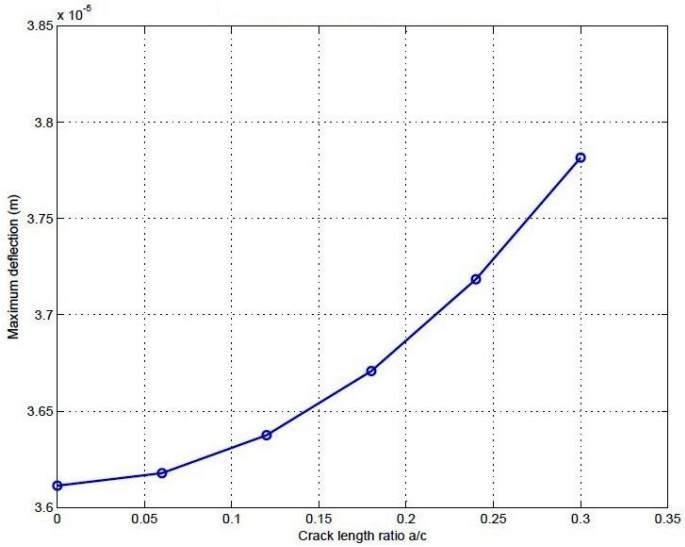

Figure 12. The static deflection of FGM plate at 1000 N concentrated load

tip. The results of KI remain around 1×10^6 Pa√m, and high accuracy is achieved. The low scatter at distances of 5-7 mm suggests that the method is not particularly sensitive to distance r, thereby increasing reliability. What was imposed at all should be compared, and they should be consistent and have a constant value ≤10 4 2.4. In summary, the findings verify that the numerical methodology for fracture analysis of cracked structures is reliable and that the approach is a safe and efficient way to determine mode I SIFs.

4.4 Static, harmonic and transient results examples

Fig. 12 presents the static deflection of the FGM plate under a 1000 N concentrated load. The

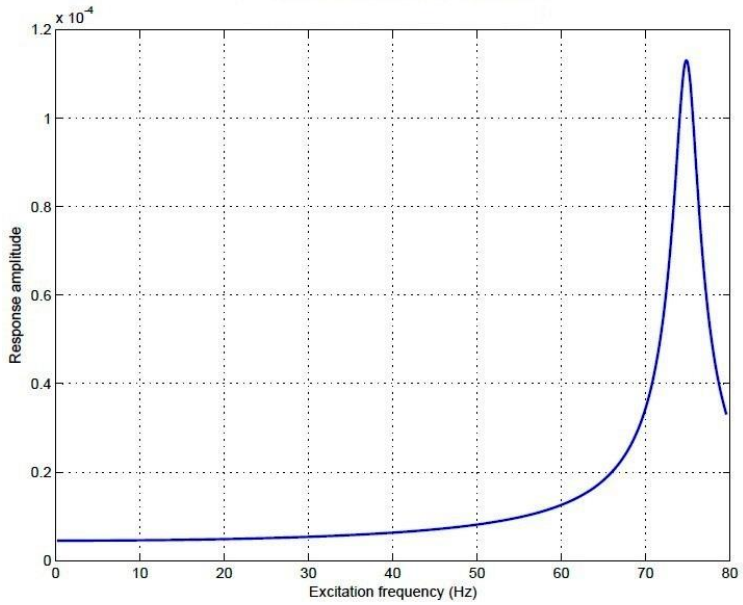

Figure 13. Harmonic response of a cracked functionally graded material (FGM) plate at a damping ratio of zeta=0.02, *k*=2, crack length=0.2, and fundamental frequency mode (1,1)

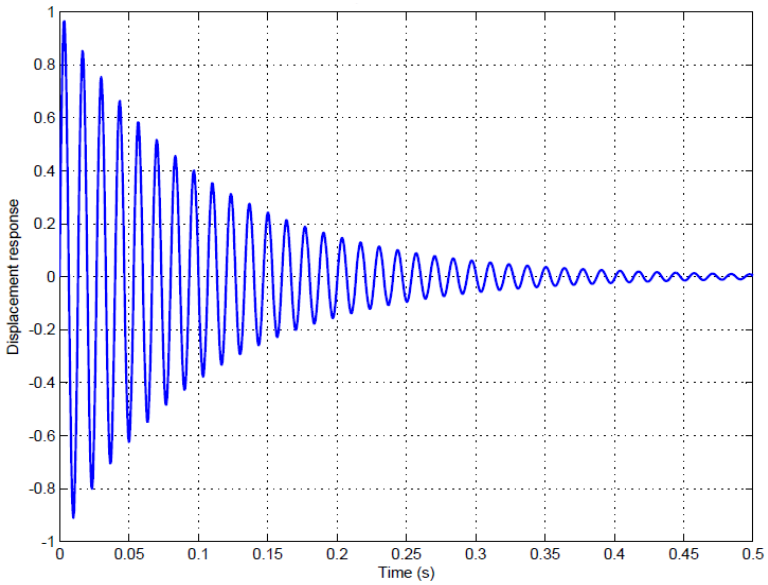

Figure 14. Transient response of a cracked functionally graded material (FGM) plate under specified conditions. Parameters: *k*=2, crack length=0.2, *a*=1 m, *b*=1 m, *h*=0.01 m

results indicate that static deflection increases significantly with greater crack length, attributed to reduced effective bending stiffness. This sensitivity demonstrates that static response serves as a reliable global damage indicator in FGM plates. The findings underscore the effectiveness of deflection-based structural health monitoring (SHM) for detecting stiffness degradation.

Fig. 13 displays the harmonic response of a cracked FGM plate at a damping ratio of zeta=0.02, *k*=2, crack length=0.2, and fundamental frequency (1,1). The resonance peak shifts to lower frequencies as the crack length increases, a decrease in stiffness. Amplitude amplification near resonance improves damage sensitivity, establishing harmonic response analysis as a highly effective method for structural health monitoring. This behavior facilitates crack detection through frequency-domain monitoring.

Fig. 14 presents the transient response of a cracked FGM plate at *k*=2, crack length=0.2, *a*=1 m, *b*=1 m, and *h*=0.01 m. The curve shows that the transient response decays faster and has a lower oscillation frequency as the crack length increases. These time-domain characteristics indicate energy dissipation and stiffness loss resulting from damage. Such transient signatures are especially valuable for impact-based structural health monitoring applications.

5. Conclusions

Vibration-based analysis of cracked single-phase porous functionally graded plates is conducted using the First-Order Shear Deformation Theory framework. Structural health monitoring (SHM) of functionally graded (FG) plates reveals that both crack length and orientation significantly affect vibrational behavior and structural integrity. Increasing crack length leads to a marked decrease in natural frequencies, indicating reduced global stiffness. Crack orientation, particularly at oblique angles such as 45°, produces asymmetric stress distributions and more pronounced alterations in mode shapes compared to cracks aligned with principal directions. These variations in frequency and mode shape, which are established indicators of damage, support the reliability of vibration-based assessment methods. The non-uniform material distribution in FG plates further amplifies sensitivity to defects, making modal parameters effective for early damage detection and localization. Results indicate that material gradation and porosity substantially influence the dynamic response of functionally graded material (FGM) plates, resulting in significant variations in natural frequencies. The presence of cracks causes localized stiffness degradation, leading to measurable frequency reductions that the proposed formulation accurately captures. The finite element approach adopted provides an accurate and computationally efficient means of modeling cracked FGM plates. These findings demonstrate the potential of the proposed method for SHM, as changes in global dynamic characteristics can serve as reliable indicators of damage. Furthermore, the results emphasize the need to integrate vibration-based SHM techniques into the design and maintenance of FG structures, especially in aerospace, marine, and mechanical applications where reliability is paramount. However, the most important conclusions are as follows:

1. Cracks reduce the natural frequencies of porous functionally graded material (FGM) plates by approximately 10-12% for a/c=0.3 at θ=0°, which indicates substantial stiffness degradation when cracks are aligned longitudinally.
2. The reduction in frequency depends strongly on crack orientation. Cracks aligned at 0° cause the greatest decrease, while cracks at 90° result in a much smaller reduction, typically less than 5 percent. This demonstrates pronounced directional sensitivity.
3. The proposed first-order shear deformation theory (FSDT) model, which incorporates the stiffness-reduction factor β, predicts the frequencies of cracked plates with less than 1% (at a/c=0.01, θ= 0°, 45°, and 90°) deviation from ANSYS results. This accuracy validates the model's suitability for vibration-based structural health monitoring (SHM) applications.

Although the proposed formulation demonstrates effectiveness, this study has several limitations. The analysis is confined to linear free vibration behavior and employs idealized crack modeling based on stiffness reduction, without explicit consideration of crack propagation or nonlinear damage mechanisms. Furthermore, thermal effects, material uncertainty, and environmental variability are not incorporated, even though these factors may affect the dynamic response of functionally graded material (FGM) structures in real-world applications. Likewise, this study utilizes an equivalent stiffness reduction approach and assumes linear material behavior, which may not adequately represent crack breathing, nonlinear dynamics, or high-amplitude loading effects. Subsequent research will address these limitations by developing fully coupled finite element method-structural health monitoring (FEM-SHM) frameworks that incorporate nonlinear crack models, damping identification, experimental validation, and real-time damage detection through multi-physics and data-driven methodologies.

Future research could extend the current framework by incorporating nonlinear vibration and transient dynamic analyses, advanced crack representations, and experimental validation to improve reliability. Additionally, integrating the proposed model with data-driven or machine learning-based damage identification techniques may enhance its applicability in real-time structural health monitoring systems for functionally graded structures.

References

1. Ezard, B., Li, L., Hao, H., Wang, R., An, S. (2025). Robust structural damage detectionwithdeep multiple instance learning for sensor fault tolerance. Engineering Structures, 331, 119957. https://doi.org/10.1016/j.engstruct.2025.119957.
2. Wang, Z., Shi, H., Dong, Z., Wen, X., Jia, W., Zhang, R. (2025). Refined frequency monitoring based on characteristic excitation with application to early fault diagnosis of thin plate damage. Mechanical Systems and Signal Processing, 228, 112432. https://doi.org/10.1016/j.ymssp.2025.112432.
3. Pérez-Aranda, C., Rivero-Ayala, M., Falla, C., Gamboa, F., Avilés, F. (2025). Electrical monitoring of structural health of laminated composite panels under compressive loading using carbon nanotube yarns. Composites Communications, 59, 102565. https://doi.org/10.1016/j.coco.2025.102565.
4. Jirawattanasomkul, T., Hang, L., Srivaranun, S., Likitlersuang, S., Jongvivatsakul, P., Yodsudjai, W., Thammarak, P. (2025). Digital twin-based structural health monitoring and measurements of dynamic characteristics in balanced cantilever bridge. Resilient Cities and Structures, 4(3), 48-66. https://doi.org/10.1016/j.rcns.2025.08.001.
5. Abdulmajeed, A., Najim, E., AlMaliky, F.T., Madan, R. (2026). Vibration analysis of stiffened composite plates reinforced by nano materials: analytical and experimental investigations. Journal of Computational Applied Mechanics, 57(2), 257-274. https://doi.org/10.22059/jcamech.2025.408569.1746.
6. Nayeeif, A.A., Al-Ameen, E.S., Jebur, N.A., Farhan Ogaili, A.A., Hamdan, Z.K., Njim, E.K. (2025). Investigation of the effects of unbalance and bearing wear on shaft vibration in a natural gas turbine plant. Applied Science and Engineering Progress, 18(4), 7863. https://doi.org/10.14416/j.asep.2025.07.012.
7. Abbood, M.Y., Gill, S., Uwayed, A.N., Mothanna, A., Ali, M., Njim, E.K., ... Madan, R. (2025). A study of the quasi-static and low-velocity impact behavior of laminated CFRP composites. Advances in Computational Design, 10(3), 299-320. https://doi.org/10.12989/acd.2025.10.3.320.
8. Zhu, Y., Liu, Z., Cheng, L., Lang, Z. (2024). Data-driven science and physically interpretable machine learning for complex dynamic systems. https://doi.org/10.1016/B978-0-443-14081-5.00127-6.
9. Fang, W., Duncan, M., Dua, M., Mertiny, P., Naguib, H.E. (2025). Machine learning-assisted design of multilayer thermoplastic composites: robust neural network prediction and feature importance analysis.

Macromolecular Materials and Engineering, 310(9), 70005. https://doi.org/10.1002/mame.202500093.
10. Abbas, E.N., Resan, K.K., Jweeg, M.J., Njim, E.K., Madan, R. (2026). Fabrication and experimental analysis of a novel flexible keel prosthetic foot utilizing functionally graded materials. Journal of Medical Engineering & Technology, 50(1), 56-64. https://doi.org/10.1080/03091902.2025.2570158.
11. Madan, R., Khobragade, P., Bhowmick, S. (2024). Impact of porosity on free vibration and limit analysis of power-law-based functionally graded disks. Multidiscipline Modeling in Materials and Structures, 20(6), 1192-1212. https://doi.org/10.1108/MMMS-04-2024-0108.
12. Sahu, A., Bhowmick, S. (2023). Graded longitudinal fins having spatially varying temperature-dependent thermophysical properties. Journal of Thermophysics and Heat Transfer, 37(3), 549-564. https://doi.org/10.2514/1.t6724.
13. Zouatnia, N., Hadji, L., Atmane, H. A., Nebab, M., Madan, R., Bennai, R., Dahmane, M. (2024). Analysis of free vibration in bi-directional power law-based FG beams employing RSD theory. Coupled Systems Mechanics, 13(4), 359-373. https://doi.org/10.12989/csm.2024.13.4.359.
14. Tati, A., Belounar, A., Sadgui, A. (2024). Bending and free vibration analysis of FG circular plates using a five unknown high order shear deformation theory. Mechanics Based Design of Structures and Machines, 52(10), 8116-8140. https://doi.org/10.1080/15397734.2024.2315173.
15. Bich, D.H., Dung, D.V., Hoa, L.K. (2012). Nonlinear static and dynamic buckling analysis of functionally graded shallow spherical shells including temperature effects. Composite Structures, 94(9), 2952-2960. https://doi.org/10.1016/j.compstruct.2012.04.012.
16. Sadgui, A., Tati, A. (2021). A novel trigonometric shear deformation theory for the buckling and free vibration analysis of functionally graded plates. Mechanics of Advanced Materials and Structures, 29(27), 6648-6663. https://doi.org/10.1080/15376494.2021.1983679.
17. Tati, A., Belounar, A., Sadgui, A. (2024). Bending and free vibration analysis of FG circular plates using a five unknown high order shear deformation theory. Mechanics Based Design of Structures and Machines, 52(10), 8116-8140. https://doi.org/10.1080/15397734.2024.2315173.
18. Hemalatha, K., Akshaya, A., Qabur, A., Kumar, S., Tharwan, M., Alnujaie, A., Alneamy, A. (2025). Transverse wave propagation in functionally graded structures using finite elements with perfectly matched layers and infinite element coupling. Mathematics, 13(13), 2131. https://doi.org/10.3390/math13132131.
19. Alnujaie, A., Ghazwani, M.H., Assie, A.E., Eltaher, M.A., Van Vinh, P. (2025). Damped vibration characteristics of functionally graded sandwich beams resting on an advanced viscoelastic foundation model. Acta Mechanica, 236(9), 5353-5374. https://doi.org/10.1007/s00707-025-04439-x.
20. Dahmane, M., Benadouda, M., Bennai, R., Saimi, A., Atmane, H.A. (2024). Effect of crack on the dynamic response of bidirectional porous functionally graded beams on an elastic foundation based on finite element method. Acta Mechanica, 235(6), 3849-3860. https://doi.org/10.1007/s00707-024-03906-1.
21. Nebab, M., Dahmane, M., Belqassim, A., Atmane, H.A., Bernard, F., Benadouda, M., Bennai, R., Hadji, L. (2023). Fundamental frequencies of cracked FGM beams withinfluence of porosity and Winkler/Pasternak/Kerr foundation support using a new quasi-3D HSDT. Mechanics of Advanced Materials and Structures, 31(28), 10639-10651. https://doi.org/10.1080/15376494.2023.2294371.
22. Latroch, N., Dahmane, M., Benosman, A.S., Bennai, R., Atmane, H.A., Benadouda, M. (2023). Inclined crack identification in bidirectional FG beams on an elastic foundation using the h-version of the finite element method. Mechanics of Advanced Materials and Structures, 31(28), 10477-10483. https://doi.org/10.1080/15376494.2023.2290226.
23. Kehli, A., Nebab, M., Bennai, R., Ait Atmane, H., Dahmane, M. (2024). Dynamic characteristics analysis of functionally graded cracked beams resting on viscoelastic medium using a new quasi-3D HSDT. Mechanics of Advanced Materials and Structures, 31(30), 12651-12664. https://doi.org/10.1080/15376494.2024.2326983.
24. Khaleel, H.H., Al-Hadrayi, Z.M.R. (2025). Free vibration analysis of rotating functionally graded material beams on elastic foundations using the Homotopy Perturbation Method. Mathematical Modelling of Engineering Problems, 12(8), 2771-2780. https://doi.org/10.18280/mmep.120818.
25. Tharwan, M.Y., Daikh, A.A., Assie, A.E., Alnujaie, A., Eltaher, M.A., Abdraboh, A.M. (2024). Static

behaviour of 3D porous metal foam shells. Springer Science and Business Media LLC. https://doi.org/10.21203/rs.3.rs-4213732/v1.

26. Djilali Djebbour, K., Mokhtar, N., Hassen, A.A., Alghanmi, R.A., Hadji, L., Riadh, B. (2024). An enhanced quasi-3D HSDT for free vibration analysis of porous FG-CNT beams on a new concept of orthotropic VE-foundations. Mechanics of Advanced Materials and Structures, 32(5), 893-909. https://doi.org/10.1080/15376494.2024.2356728.
27. Hameed, H., Munir, S., Zaman, F.D. (2024). Green's function coupled with perturbation approach to dynamic analysis of inhomogeneous beams with eigenfrequency and rotational effect's investigations. Structural Monitoring and Maintenance, 11(1), 19-40. https://doi.org/10.12989/smm.2024.11.1.019.
28. Xie, Y., Yan, S., Wang, Y., Song, S. (2024). Comparative research on gravity load simulation devices for structural seismic tests based on FEA. Structural Monitoring and Maintenance, 11(3), 235-246. https://doi.org/10.12989/smm.2024.11.3.235.
29. Wu, Z., Xiao, M., Sun, Y., Wang, H. (2025). Machine learning-based methodologies for probabilistic prediction of random seismic frame structural response. Structural Monitoring and Maintenance, 12(1), 71-91. https://doi.org/10.12989/smm.2025.12.1.071.
30. Neamah, R.A., Nassar, A.A., Alansari, L.S., Njim, E.K., Madan, R. (2025). Experimental and analytical investigation of free vibration of a crack FG beam reinforced with alumina nano particles. Advances in Nano Research, 18(1), 19-31. https://doi.org/10.12989/anr.2025.18.1.019.
31. Kadum Njim, E., Al-Maamori, M.H., Madan, R., Bakhy, S.H., Al-Waily, M., Khobragade, P., Hadji, L. (2025). Numerical and analytical investigation of free vibration behavior of porous functionally graded sandwich plates. Mechanics of Advanced Composite Structures, 12(3), 555-568. https://doi.org/10.22075/macs.2024.34962.1710.
32. Raad, H., Najim, E., Jweeg, M., Al-Waily, M., Hadji, L., Madan, R. (2024). Vibration analysis of sandwich plates with hybrid composite cores combining porous polymer and foam structures. Journal of Computational Applied Mechanics, 55(3), 485-499. https://doi.org/10.22059/jcamech.2024.377658.1121.
33. Daneshmand, S., Vini, M.H., Sajadi, S.M., Mouthanna, A., Jasim, D.J., Hammoodi, K.A., ... Nasajpour-Esfahani, N. (2023). Numerical and experimental investigations of mechanical, tribological, and electrical properties of laminated Bi-metal Al/SiC/Ni composites. Materials Today Communications, 37, 107355. https://doi.org/10.1016/j.mtcomm.2023.107355.
34. Hissaria, P., Ramteke, P.M., Hirwani, C.K., Mahmoud, S.R., Kumar, E.K., Panda, S.K. (2023). Numerical investigation of eigenvalue characteristics (vibration and buckling) of damaged porous bidirectional FG panels. Journal of Vibration Engineering & Technologies, 11(4), 1889-1901. https://doi.org/10.1007/s42417-022-00677-8.
35. Sinha, G.P., Kumar, B. (2021). Review on vibration analysis of functionally graded material structural components with cracks. Journal of Vibration Engineering & Technologies, 9(1), 23-49. https://doi.org/10.1007/s42417-020-00208-3.
36. Andreaus, U., Baragatti, P. (2011). Cracked beam identification by numerically analysing the nonlinear behaviour of the harmonically forced response. Journal of Sound and Vibration, 330(4), 721-742. https://doi.org/10.1016/j.jsv.2010.08.032.
37. Gupta, A., Jain, N.K., Salhotra, R., Joshi, P.V. (2018). Effect of crack location on vibration analysis of partially cracked isotropic and FGM micro-plate with non-uniform thickness: an analytical approach. International Journal of Mechanical Sciences, 145, 410-429. https://doi.org/10.1016/j.ijmecsci.2018.07.015.
38. Nasirmanesh, A., Mohammadi, S. (2017). An extended finite element framework for vibration analysis of cracked FGM shells. Composite Structures, 180, 298-315. https://doi.org/10.1016/j.compstruct.2017.08.019.
39. Zheng, H., Sladek, J., Sladek, V., Wang, S.K., Wen, P.H. (2021). Hybrid meshless/displacement discontinuity method for FGM Reissner's plate with cracks. Applied Mathematical Modelling, 90, 1226-1244. https://doi.org/10.1016/j.apm.2020.10.023.
40. Xu, A., Huang, J., Ning, R., Chen, H. (2025). Prediction of vibration energy and stress distribution in FGM plates at high-frequencies using radiative energy transfer method. Thin-Walled Structures, 215,

113444. https://doi.org/10.1016/j.tws.2025.113444.
41. Wang, C., Han, X., Yang, C., Zhang, X., Hou, W. (2020). Assumed stress quasi-conforming formulation for static and free vibration analysis of symmetric laminated plates. Engineering Computations, 37(6), 2051-2083. https://doi.org/10.1108/EC-04-2019-0179.
42. Li, C., Li, S., Zhang, Y.M., Cai, J.W., Lai, S.K. (2025). In-plane vibration analysis of elastically restrained FGM skew plates using variational differential quadrature method. Computers & Mathematics with Applications, 178, 136-153. https://doi.org/10.1016/j.camwa.2024.11.026.
43. Chung, N.T., Thuy, N.N., Thu, D.T.N., Chau, L.H. (2019). Numerical and experimental analysis of the dynamic behavior of piezoelectric stiffened composite plates subjected to airflow. Mathematical Problems in Engineering, 1, 2697242. https://doi.org/10.1155/2019/2697242.
44. Azeez Neamah, R., Ahmed Nassar, A., Alansari, L.S., Kadum Njim, E., Hadji, L., Madan, R. (2025). Static deflection analysis of functionally graded beams using various beam theories. Mathematical Modelling and Numerical Simulation with Applications, 5(2), 396-420. https://doi.org/10.53391/mmnsa.1524642.
45. Amir, M., Lim, J., Kim, S.W., Lee, S.Y. (2023), Finite element analysis of natural frequencies of the FGM porous cooling plate with cutouts: a multilayered FGM approach, Results in Engineering, 20, 101532. https://doi.org/10.1016/j.rineng.2023.101532.
46. Abd Alqader, S.Q., Bedaiwi, B.O., Njim, E.K., Takhakh, A.M., Hadji, L. (2024). Free vibration analysis for polyester/graphene nanocomposites multilayer functionally graded plates. Physics and Chemistry of Solid State, 25(4), 704-717. https://doi.org/10.15330/pcss.25.4.704-717.
47. Muthanna, A., Ali, M., Hasan, H.M., Najim, K.B., Njim, E.K., Madan, R., Al-Maamori, M.H. (2025). Vibration investigation of an imperfect FGM cylindrical shell reinforced by various types of stiffeners with temperature-dependent properties resting on an elastic foundation. Coupled Systems Mechanics, 14(2), 105-127. https://doi.org/10.12989/csm.2025.14.2.105.
48. Ellali, M., Amara, K., Bouazza, M. (2024). Thermal buckling of porous FGM plate integrated surface-bonded piezoelectric. Coupled Systems Mechanics, 13(2), 171-186. https://doi.org/10.12989/csm.2024.13.2.171.
49. Zohra, A., Rabia, B., Tahar, H.D. (2024). Study and analysis of porosity distribution effects on the buckling behavior of functionally graded plates subjected to diverse thermal loading. Coupled Systems Mechanics, 13(2), 115-132. https://doi.org/10.12989/csm.2024.13.2.115.
50. Rubine, L., Selvamani, R., Ebrahimi, F. (2024). Nonlinear thermal vibration of fluid infiltrated magneto piezo electric variable nonlocal FG nanobeam with voids. Coupled Systems Mechanics, 13(4), 337-357. https://doi.org/10.12989/csm.2024.13.4.337.
51. Tayeb, B., Abderezak, R., Daouadji, T.H. (2024). Mechanical behavior of composite beam aluminum-sandwich honeycomb strengthened by imperfect FGM plate under thermo-mechanical loading. Coupled Systems Mechanics, 13(2), 133-151. https://doi.org/10.12989/csm.2024.13.2.133.
52. Huang, X.L., Shen, H.S. (2004). Nonlinear vibration and dynamic response of functionally graded plates in thermal environments. International Journal of Solids and Structures, 41(9), 2403-2427. https://doi.org/10.1016/j.ijsolstr.2003.11.012.
53. Victor, I., Holm, A. (2024). Effect of longitudinal cracks on structural life of functionally graded beams exhibiting creep. Structural Monitoring and Maintenance, 12(4), 355-375. https://doi.org/10.12989/smm.2025.12.4.355.
54. Avcar, M. (2019). Free vibration of imperfect sigmoid and power law functionally graded beams. Steel and Composite Structures, 30(6), 603-615. https://doi.org/10.12989/scs.2019.30.6.603.
55. Arefi, M., Kiani, M., Zamani, M. (2020). Nonlocal strain gradient theory for the magneto-electro-elastic vibration response of a porous FG-core sandwich nanoplate with piezomagnetic face sheets resting on an elastic foundation. Journal of Sandwich Structures & Materials, 22(7), 2157-2185. https://doi.org/10.1177/1099636218795378.
56. Alhous, Z.F.A., Jweeg, M.J., Njim, E.K., Mouthanna, A., Flayyih, M.A., Madan, R., Khobragade, P., Rai, P.K. (2025). Nonlinear frequency and dynamic response of PLA polymeric imperfect FG sandwich plates under hygrothermal conditions. Coupled Systems Mechanics, 14(1), 1-19. https://doi.org/

10.12989/csm.2025.14.1.001.
57. Reddy, J.N. (1984). A simple higher-order theory for laminated composite plates. Journal of Applied Mechanics, 51(4), 745-752. https://doi.org/10.1115/1.3167719.

Nomenclature

Symbol	Describtion	Unit
a,b	Plate length and width	m
h	Plate thickness	m
x,y,z	Cartesian coordinates	m
c	ceramic	
m	metal	
V_c	volume fraction of ceramic	-
V_m	volume fraction of metal	-
u_o,v_o	Mid-plane in-plane displacements	m
Φ_x, Φ_y	Rotations of normal about yyy- and xxx-axes	rad
$\varepsilon_x,\varepsilon_y$	Normal strains	-
γ_{xy}	In-plane shear strain	-
γ_{xz},γ_{yz}	Transverse shear strains	-
$E(z)$	Effective Young's modulus (FGM)	Pa
E_m, E_c	Young's modulus of metal and ceramic	Pa
v	Poisson's ratio	-
$\rho(z)$	Density through thickness	kg/m^3
ρ_m,ρ_c	Density of metal and ceramic	kg/m^3
k	Power-law index	-
$C_{i,j}$	Reduced stiffness coefficients	-
w	The deflection of the panel	m
t	time	s
w_o	Mid-plane transverse displacement	m
k_s	Shear correction factor	m
N_x,N_y,N_{xy}	In-plane force resultants	N/m
I_0	Mass per unit area	kg/m²
I_2	Rotary inertia term	kg·m²/m²
$[K]$	Global stiffness matrix	N/m
$[M]$	Global mass matrix	kg
$q(x,y)$	Transverse distributed load	N/m²
P	Concentrated load	N
ω	Natural circular frequency	rad/s
Φ	Mode shape vector	-
β	Crack stiffness reduction factor	-
a (*crack*)	Crack length	m
θ	Crack orientation angle	rad or °
Ω	Plate mid-surface domain	m²
α	stiffness degradation parameter	-